ChemPubSoc Europe

DOI: 10.1002/cssc.201500490

CHEMSUSCHEM Communications

A Bioinspired Molecular Polyoxometalate Catalyst with Two Cobalt(II) Oxide Cores for Photocatalytic Water Oxidation

Jie Wei,[a] Yingying Feng,[a] Panpan Zhou,[a] Yan Liu,[a] Jingyin Xu,[a] Rui Xiang,[a] Yong Ding,*[a, b] Chongchao Zhao,[c] Linyuan Fan,[d] and Changwen Hu[d]

To overcome the bottleneck of water splitting, the exploration of efficient, selective, and stable water oxidation catalysts (WOCs) is crucial. We report an all-inorganic, oxidatively and hydrolytically stable WOC based on a polyoxometalate $[(A\text{-}\alpha\text{-}SiW_9O_{34})_2Co_8(OH)_6(H_2O)_2(CO_3)_3]^{16-}$ (Co_8POM). As a cobalt(II)-based cubane water oxidation catalyst, Co_8POM embeds double $Co^{II}_4O_3$ cores. The self-assembled catalyst is similar to the oxygen evolving complex (OEC) of photosystem II (PS II). Using $[Ru(bpy)_3]^{2+}$ as a photosensitizer and persulfate as a sacrificial electron acceptor, Co_8POM exhibits excellent water oxidation activity with a turnover number (TON) of 1436, currently the highest among bioinspired catalysts with a cubical core, and a high initial turnover frequency (TOF). Investigation by several spectroscopy, spectrometry, and other techniques confirm that Co_8POM is a stable and efficient catalyst for visible light-driven water oxidation. The results offer a useful insight into the design of water oxidation catalysts.

Splitting water into H_2 and O_2 through artificial photosynthesis is a feasible way to alleviate the energy crisis in the future.[1] To break through the bottleneck of water splitting, the exploration of efficient, selective, and stable water oxidation catalysts (WOCs) is crucial.[2] Nature's cuboidal $CaMn_4O_5$ catalyst of photosystem II (PS II) is the heuristic component for design of bioinspired WOCs, and the transition-metal-oxo cubical core has been recognized as being of critical importance towards catalysis of water oxidation.[3]

In order to closely mimic the structure of the cubical core, many efforts have been devoted to exploring cubical tetranuclear metal catalysts.[4] However, only few molecular tetranuclear metal catalysts, including ruthenium-,[5] manganese-,[6] cobalt-,[3,7] and nickel-based[8] complexes, have so far been synthesized and recognized as viable WOCs under photocatalytic conditions. Within the scope of metal organic complexes, just three typical examples have been reported: $[Co^{III}_4O_4(OAc)_4(py)_4]$,[3] $[Co^{III}_4O_4(OAc)_4(p\text{-}NC_5H_4X)_4]$ (where X = H, Me, *t*Bu, OMe, Br, OAc, CN),[7a] and $[Co^{II}_4(hmp)_4(\mu\text{-}OAc)_2(\mu_2\text{-}OAc)_2(H_2O)_2]$.[7b] Nevertheless, Nocera et al. recently raised doubts about whether or not catalyst $[Co^{III}_4O_4(OAc)_4(py\text{-}X)_4]$ mentioned above is a genuine molecular catalyst in photocatalytic water oxidation.[9] The result of their research is that the water oxidation activity of the compound class $[Co^{III}_4O_4(OAc)_4(py\text{-}X)_4]$ emanated from Co^{II} impurities. A possible reason why the $[Co^{III}_4O_4(OAc)_4(py\text{-}X)_4]$ is not responsible for the observed water oxidation activity is that structure of compound class $[Co^{III}_4O_4(OAc)_4(py\text{-}X)_4]$ contains no terminal aquo ligands. Inspired by the proposed PS II–oxygen evolution complex (OEC) mechanisms, the implementation of transition metals coordinated to terminal aquo, hydroxo, or oxo ligands is a major step toward O–O formation pathways via water attack and exchange processes.[10]

Recently, many robust, molecular polyoxometalates (POMs) as efficient WOCs have been developed, because this kind of catalyst eliminates the problem of ligand oxidative instability, while being thermally stable and allowing for structural fine-tuning.[5–6,7c,11] However, apart from $[\{Ru_4O_4(OH)_2\text{-}(H_2O)_4\}(\gamma\text{-}SiW_{10}O_{36})_2]^{10-}$, based on a noble metal,[5] only three types of bioinspired POMs containing earth-abundant metals with cubical core have been reported: $[\{Co_4(OH)_3(PO_4)\}_4(XW_9O_{34})_4]^{n-}$ (X = Si, P, Ge, As),[7c] $[Mn_4O_3(CH_3COO)_3(A\text{-}\alpha\text{-}SiW_9O_{34})]^{6-}$,[6] and $[Ni_{25}(H_2O)_2\text{-}OH)_{18}(CO_3)_2(PO_4)_6(SiW_9O_{34})_6]^{50-}$.[8] The lack of transition metals coordinated to a terminal aquo ligand in the first two catalysts mentioned above may result in a lower turnover number (TON). The number of fast, selective, and stable molecular POMs that function as WOCs is still small up to now.

Herein, we report the synthesis, crystal structure, and photocatalytic water oxidation activity of a homogeneous POM WOC, $[(A\text{-}\alpha\text{-}SiW_9O_{34})_2Co_8(OH)_6(H_2O)_2(CO_3)_3]^{16-}$. This octanuclear cobalt complex contains double-defective cubical $Co^{II}_4O_3$ cores (Figure 1), with two of these cobalt atoms coordinated to ter-

[a] J. Wei, Y. Feng, P. Zhou, Y. Liu, J. Xu, R. Xiang, Prof. Dr. Y. Ding
Key Laboratory of Nonferrous Metal Chemistry and Resources Utilization of GanSu Province
State Key Laboratory of Applied Organic Chemistry
College of Chemistry and Chemical Engineering
Lanzhou University
Lanzhou 730000 (PR China)
E-mail: dingyong1@lzu.edu.cn

[b] Prof. Dr. Y. Ding
State Key Laboratory for Oxo Synthesis and Selective Oxidation
Lanzhou Institute of Chemical Physics
Chinese Academy of Sciences
Lanzhou 730000 (PR China)

[c] C. Zhao
Department of Chemistry
Northwestern University
Evanston, IL, 60201 (USA)

[d] L. Fan, C. Hu
Key Laboratory of Cluster Science Ministry of Education
Beijing Key Laboratory of Photoelectronic/Electrophotonic
School of Chemistry, Beijing Institute of Technology
Beijing 100081 (PR China)

Supporting Information for this article is available on the WWW under http://dx.doi.org/10.1002/cssc.201500490.

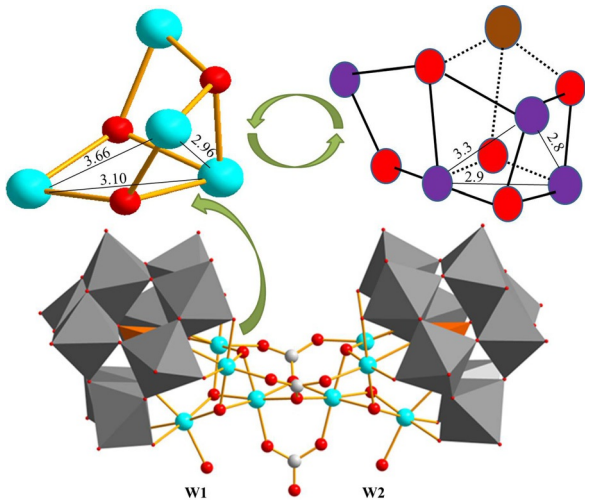

Figure 1. Combined polyhedral/ball-and-stick representation of Co_8POM (bottom: Co, cyan; O, red; Si, orange; C, white; W, gray; counter cations and H atoms were omitted for clarity) and Mn_4CaO_5 (top: Mn, violet; Ca, brown; O, red).

minal aquo ligands.[12] Co_8POM is readily synthesized from $Na_{10}[A\text{-}\alpha\text{-}SiW_9O_{34}]$, $CoSO_4$, and potassium carbonate in an aqueous solution of sodium acetate at room temperature (see Supporting Information for details). After potassium carbonate solution was added and stirring for 1 h at room temperature, the resulting solution was maintained at pH 9.0 all the time. It is well-known that POMs are hydrolytically sensitive, especially under alkaline conditions.[2b] Co_8POM was synthesized at pH around 9.0, which can insure its hydrolytic stability during the process of photocatalytic water oxidation at pH 9.0. The hydrolytic stability of Co_8POM in 80 mM pH 9.0 sodium borate buffer was further confirmed by UV/Vis experiments (Supporting Information, Figures S5 and S7).

Purple, platelike crystals of Co_8POM were obtained (Supporting Information, Figure S2), and the crystal structure was triclinical (Supporting Information, Table S1). As can be seen from this POM (Supporting Information, Figure S1), two $Co^{II}_4O_3$ cores are located in two trivacant $[A\text{-}\alpha\text{-}SiW_9O_{34}]^{10-}$ ligands and are connected by three CO_3^{2-} anions (Supporting Information, Figure S3). All the Co–O bond lengths fall into 2.0–2.4 Å (Supporting Information, Table S2), and the $Co^{II}\cdots Co^{II}$ distances of the $Co^{II}_4O_3$ cores are in the range of 2.96–3.75 Å (Supporting Information, Table S3). These structural features show a direct relationship to the $CaMn_4O_5$ cubane of Nature's PS II, where Mn···Mn distances fall in the range of 2.8–3.3 Å (Figure 1).[13,14] Bond valence sum (BVS) calculations indicate that all the cobalt atoms in the Co_8POM have a +2 oxidation state (Supporting Information, Table S4); a finding supported by X-ray photoelectron spectroscopy results (Supporting Information, Figure S8).[7c,11h,15]

The UV/Vis spectrum of Co_8POM in 80 mM borate buffer reveals transitions involving orbitals with both cobalt and polyoxometalate ligand character. An intense band around 508 nm ($\varepsilon_{480} = 184\ M^{-1}\,cm^{-1}$, $\varepsilon_{508} = 190\ M^{-1}\,cm^{-1}$) in the UV/Vis spectrum of Co_8POM in solution (Figure S5) is in good agreement with other Co^{II}-containing polyoxometalates.[16] DFT calculations further revealed the electronic properties of Co_8POM. An optimized geometry of Co_8POM is presented in Figure S11 (Supporting Information), and the calculated important bond distances are in good agreement with the X-ray crystallographic values. The highest occupied molecular orbital (HOMO) of Co_8POM is mostly cobalt core orbital (Supporting Information, Figure S12). These results indicate that the $\{Co_4O_3\}$ units should participate in the water oxidation reaction whereas polytungstate ligands and carbonate ligands should be effectively inert under the catalytic conditions. Furthermore, in the oxidative scan, cyclic voltammetry (CV) of 0.5 mM Co_8POM in 80 mM sodium borate buffer solution (pH 9.0) shows a large, irreversible oxidative wave corresponding to catalytic water oxidation with an onset potential of 0.95 V (vs. Ag/AgCl (saturated KCl), Supporting Information, Figure S13).

Photoinduced water oxidation was investigated using a sacrificial system, which was composed of $[Ru(bpy)_3]^{2+}$ (1 mM), $Na_2S_2O_8$ (5 mM), borate buffer solution (80 mM, pH 9.0, 15 mL), and excited at $\lambda \geq 420$ nm. Figure 2 shows the oxygen evolution over Co_8POM under different pH conditions. Oxygen production leveled off to a plateau yield after 9 min of irradiation due to the consumption of electronic sacrificial reagent ($S_2O_8^{2-}$). Because a high pH is thermodynamically favorable for water oxidation,[17] the reaction at pH 9.0 showed a higher catalytic activity with 43.6% O_2 yield and TON of 545. When the pH 8.0 buffer was used, the O_2 yield and TON decreased to 20.5% and 256, respectively. After completion of the first run, 17.8 mg $Na_2S_2O_8$ was added to the reaction and the system started producing oxygen again (Supporting Information, Figure S14, Table S6). In the second run, the amount of O_2 decreased from 16.4 μmol to 8.4 μmol and O_2 yield decreased from 43.6% to 22.4%, respectively. At the same time, the pH value was 8.7 after the first run, and changed to 8.0 after the second run. These phenomena suggest that the photocatalytic reaction system is influenced by the pH value. In addition, the decomposition of photosensitizer $[Ru(bpy)_3]^{2+}$ also influences the photocatalytic reaction.

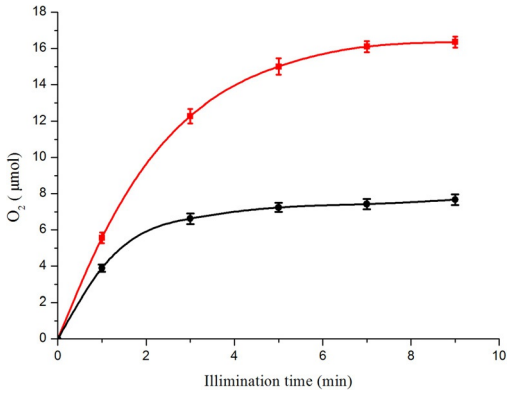

Figure 2. Kinetics of O_2 production in the photocatalytic system by 2 μM Co_8POM under different pH conditions in 80 mM borate buffers (black curve at pH 8 and red curve at pH 9) containing $[Ru(bpy)_3]^{2+}$ (1 mM) and $Na_2S_2O_8$ (5 mM).

Light-driven water oxidation activity was also examined at different concentrations of Co_8POM (Supporting Information, Table S5). The TON of Co_8POM reached as high as 1436 using 0.5 μM catalyst. The quantum yield of the photoinduced reaction is directly related to the initial slope (O_2 versus time), which can reach as high as ~36% at 2.0 μM Co_8POM. In order to differentiate homogeneous and heterogeneous water oxidation catalysis, the photocatalytic water oxidation activity of Co_8POM and $Co(NO_3)_2$ (in situ-generated cobalt oxide) were investigated thoroughly. Although water oxidation catalyzed by Co_8POM and $Co(NO_3)_2$ in separate reactions exhibited similar kinetic profiles, more oxygen evolved when using $Co(NO_3)_2$ at both pH 8.0 and pH 9.0 (this phenomenon is common[11i]) (Supporting Information, Figure S15). On the other hand, Co_8POM was proved to have a higher activity at pH 5.8 (Supporting Information, Figure S16). The difference in catalytic water oxidation activity at different pH values using Co_8POM or the equivalent Co^{2+} (aq) is a strong evidence that Co_8POM is a genuine water oxidation catalyst, rather than Co^{2+} (aq) or CoO_x. Furthermore, the dependence of the catalytic water oxidation activity by Co_8POM and Co^{2+} (aq) as a function of pH and buffer concentration is different (Supporting Information, Table S6). Table S6 also gives many additional results to verify that Co_8POM is a genuine water oxidation catalyst.

$$[Ru(bpy)_3]^{2+} + hv \rightarrow *[Ru(bpy)_3]^{2+} \quad (1)$$

$$2\,*[Ru(bpy)_3]^{2+} + S_2O_8^{2-} \rightarrow 2\,[Ru(bpy)_3]^{3+} + 2\,SO_4^{2-} \quad (2)$$

$$n\,[Ru(bpy)_3]^{3+} + Co_8POM \rightarrow n\,[Ru(bpy)_3]^{2+} + Co_8POM^{(OX)} \quad (3)$$

$$Co_8POM^{(OX)} + 2\,H_2O \rightarrow Co_8POM + O_2 + 4\,H^+ \quad (4)$$

In a photoinduced sacrificial system comprising $[Ru(bpy)_3]^{2+}$ and $Na_2S_2O_8$, the photosensitizer can be oxidized to $[Ru(bpy)_3]^{3+}$ by $Na_2S_2O_8$ under photoirradiation [Eqs. (1)–(2)]. Steady-state luminescence spectra of $[Ru(bpy)_3]^{2+}$ show that 63% of the excited state $*[Ru(bpy)_3]^{2+}$ can be quenched by persulfate by comparing the emission intensity values in the presence and absence of persulfate (Supporting Information, Figure S18). Upon addition of the catalyst, the quenching efficiency is not affected, indicating that the quenching of $*[Ru(bpy)_3]^{2+}$ by Co_8POM is negligible. The resulting $[Ru(bpy)_3]^{3+}$ can further oxidize water to produce O_2 thermodynamically, but with a poor selectivity and at a lower rate.[18] However, water oxidation catalysts can break the limitations of kinetics, restoring $[Ru(bpy)_3]^{3+}$ quickly to $[Ru(bpy)_3]^{2+}$ and oxidizing water to oxygen at the same time [Eqs. (3)–(4)]. In the meantime, the WOCs can alleviate degradation of the photosensitizer, which occurs in the reduction of $[Ru(bpy)_3]^{3+}$ to $[Ru(bpy)_3]^{2+}$.[18,19] The ligand-to-metal charge transfer (LMCT) band of $[Ru(bpy)_3]^{3+}$ at 670 nm was not observed in the presence of Co_8POM in pH 8.0 borate buffer solution after 30 s of irradiation, but was obvious in the absence of catalyst (Supporting Information, Figure S19). The difference in degradation of the photosensitizer should be caused by electron transfer between $[Ru(bpy)_3]^{3+}$ and Co_8POM.

In photocatalytic cycles, the overall efficiency of oxygen production is strongly affected by the electron transfer rate from the catalyst to the oxidized photosensitizer [Eq. (3)].[4b] A fast electron transfer process between the chemical oxidant and the catalyst could contribute to a high turnover frequency (TOF) for Co_8POM in water oxidation processes. A classical experiment for investigating hole scavenging rates is flash photolysis, in which a suitable concentration of $[Ru(bpy)_3]^{3+}$ is generated by the activated reaction of $[Ru(bpy)_3]^{2+}$ with $S_2O_8^{2-}$ using a 450 nm laser. The reaction condition of $[Ru(bpy)_3]^{3+}$ with Co_8POM was monitored by detecting the absorption at 450 nm (the metal-to-ligand charge transfer (MLCT) band of $[Ru(bpy)_3]^{2+}$) due to the regeneration of $[Ru(bpy)_3]^{2+}$ [Eq. (3)]. Figure 3 shows the results obtained from the flash photolysis

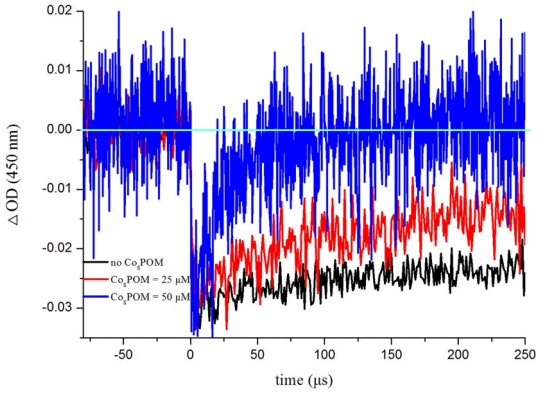

Figure 3. Laser flash photolysis experiments (λ_{exc} = 450 nm) at pH 9.0 (80 mM sodium borate buffer solution) containing $[Ru(bpy)_3]^{2+}$ (50 μM), Co_8POM (0–50 μM) and $S_2O_8^{2-}$ (5 mM).

(excitation with 450 nm light) in pH 9.0 sodium borate buffer solution with different concentrations of Co_8POM (0–50 μM) containing 50 μM $[Ru(bpy)_3]^{2+}$ and 5 mM $S_2O_8^{2-}$. The black trace shows the bleach persistence (i.e., constant $[Ru(bpy)_3]^{3+}$ concentration) obtained in the absence of Co_8POM. The presence of Co_8POM leads to bleach recovery, resulting from $[Ru(bpy)_3]^{3+}$ reduction by hole scavenging. The hole-scavenging activity increases with an increase in concentration of Co_8POM in microsecond time scale. However, these mechanisms are still not clarified because of the complexity of WOCs and the water oxidation process itself [Eqs. (3)–(4)]. In any case, the fast hole scavenging processes involving Co_8POM would allow protection towards the stability of the overall photochemical water oxidation process, because the $[Ru(bpy)_3]^{3+}$ should be rapidly scavenged and therefore could not be affected by the decomposition reaction.[18,19]

The reaction rate of $[Ru(bpy)_3]^{3+}$ reduction to $[Ru(bpy)_3]^{2+}$ is so fast at pH 9.0[11k] that monitoring the reaction conditions is difficult. Therefore, we synthesized $Ru(bpy)_3(ClO_4)_3$ and measured kinetics of $[Ru(bpy)_3]^{3+}$ reduction to $[Ru(bpy)_3]^{2+}$ at a modest overpotential of 350 mV ($\varepsilon^0([Ru(bpy)_3]^{3+}/[Ru(bpy)_3]^{2+}) = 1.24$ V, $\varepsilon^0(O_2/H_2O) = 0.89$ V at pH 5.8). In 20 mM $NaHCO_3/Na_2SiF_6$ buffer at pH 5.8, the addition of 2.0 μM Co_8POM results in ~13% conversion of $[Ru(bpy)_3]^{3+}$ in 30 s, and the conversion of

$[Ru(bpy)_3]^{3+}$ increases to ~37% with the concentration of Co_8POM increasing to 4.0 μM (Supporting Information, Figure S20). These results also demonstrate that Co_8POM can make $[Ru(bpy)_3]^{3+}$ restore to $[Ru(bpy)_3]^{2+}$ faster and break the dynamic limitation of water oxidation (Eqs. (3)–(4)).

The stability of Co_8POM was indicated by several experiments. After aging 10 h, no apparent changes in the UV/Vis spectra were observed in borate buffer (Figure S7). The FTIR spectrum of the recovered catalyst after the first run was compared with that of the fresh Co_8POM, and the consistency certified structural integrity of Co_8POM (Supporting Information, Figure S21). Dynamic light scattering (DLS) measurements did not reveal nanoparticles after photocatalytic water oxidation (Supporting Information, Figure S22). However, nanoparticles (ca. 77.9 nm in diameter) were detected when using 2 μM $Co(NO_3)_2$, as shown in Figure S23 (Supporting Information). This provides solid evidence that cobalt hydroxide/oxide nanoparticles are not generated in situ from the hydrolytic decomposition of Co_8POM. Mass spectrometry analysis of Co_8POM was performed before and after the reaction, and the results show the integrity of Co_8POM polyanions after photocatalystic water oxidation (Supporting Information, Figure S24). The condition of Co_8POM before and after the photocatalytic water oxidation was investigated by X-ray photoelectron spectroscopy (XPS). The absence of changes in the surface conditions of the solid Co_8POM indicates that the structure of Co_8POM was maintained during photocatalytic water oxidation (Figure S8). These findings indicate that Co_8POM is a stable molecular catalyst in photochemical water oxidation.

The design concept behind bioinspired homogeneous WOCs is to imitate the configuration of the OEC in PS II as much as possible. This bioinspired double cubane $Co^{II}_4O_3$ core POM possesses four absolute advantages. Firstly, Co_8POM inherited the versatile nature of POMs. This family of catalysts can readily withstand highly oxidizing conditions, while allowing structural fine-tuning and showing thermal stability. Secondly, two unique tetracobalt cores are stabilized by a hybrid set of ligands, including two all-inorganic tungstosilicate platform and three carbonate ligands. Carbonate ligands endow the Co_8POM both flexibility and the hydrolytic stability over a higher pH range. The $Co^{II}_4O_3$ core in Co_8POM is similar to the PS II–OEC. Thirdly, except for the organometallic compound $[Co^{II}_4(hmp)_4(\mu\text{-}OAc)_2(\mu_2\text{-}OAc)_2(H_2O)_2]$,[7b] the first realization of aquo ligands in synthetic cubane POMs based on abundant metals is a significant step toward O–O formation pathways.[10] Finally, Co_8POM exhibits excellent water oxidation activity and the highest TON within the scope of bioinspired polynuclear transition metal WOCs (Table 1). Compared to other POM WOCs, Co_8POM also shows excellent reactivity (Table S7).

In conclusion, we report that the bioinspired polyoxometalate $[(A\text{-}\alpha\text{-}SiW_9O_{34})_2Co_8(OH)_6(H_2O)_2(CO_3)_3]^{16-}$ is an active homogeneous molecular water oxidation catalyst that exhibits high hydrolytic stability and has a very high turnover number (1436). The unique $Co^{II}_4O_3$ core provides a commendable biomimetic case for new structural models to catalyze water oxidation based on the design concept of the oxygen evolving complex in photosystem II.

Table 1. TON and $TOF_{initial}$ of different water oxidation catalysts with cubical core.

Catalyst	TON[a]	TOF [s^{-1}]	Ref
Co_8POM[b]	1436	10	this work
$[Co^{III}_4O_4(OAc)_4(py)_4]$[c]	40	0.02	[3]
$[Co^{III}_4O_4(OAc)_4(p\text{-}C_5H_4X)_4]$[c]	10	0.02	[7a]
$[Co^{II}_4(hmp)_4(\mu\text{-}OAc)_2(\mu_2\text{-}OAc)_2(H_2O)_2]$[c]	40	7	[7b]
$[\{Ru_4O_4(OH)_2(H_2O)_4\}(\gamma\text{-}SiW_{10}O_{36})_2]^{10-}$[d]	500	0.1	[5a]
$[Mn^{III}_3Mn^{IV}O_3(CH_3COO)_3(A\text{-}\alpha\text{-}SiW_9O_{34})]^{6-}$[c]	5	No data	[6]
$[\{Co_4(OH)_3(PO_4)\}4(GeW_9O_{34})_4]^{32-}$[c]	70	0.1	[7c]
$[Ni_{25}(H_2O)_2OH)_{18}(CO_3)_2(PO_4)_6(SiW_9O_{34})_6]^{50-}$	25	0.3	[8]
PS II[e]	10^7	500	[20]

[a] TON = mole of O_2/mole of catalyst. [b] Conditions: LED light (16 mW, $\lambda \geq 420$ nm, beam diameter 2 cm), $[Ru(bpy)_3]Cl_2$ (1.0 mM), $Na_2S_2O_8$ (5.0 mM), Co_8POM (0.5 μM), borate buffer (80 mM, initial pH 9.0). [c] $[Ru(bpy)_3]^{2+}/S_2O_8^{2-}$. [d] Ce^{IV}-driven. [e] Tyrosine radical.

Acknowledgements

This work was financially supported by the National Natural Science Foundation of China (grant 21173105). We gratefully thank Prof. Pierre Mialane's suggestion for synthesis of cobalt polyoxometalates.

Keywords: cobalt · homogeneous catalysis · photocatalysis · polyoxometalates · water oxidation

[1] N. S. Lewis, D. G. Nocera, *Proc. Natl. Acad. Sci. USA* **2006**, *103*, 15729–15735.

[2] a) C. W. Cady, R. H. Crabtree, G. W. Brudvig, *Coord. Chem. Rev.* **2008**, *252*, 444–455; b) M. D. Karkas, O. Verho, E. V. Johnston, B. Akermark, *Chem. Rev.* **2014**, *114*, 11863–12001.

[3] N. S. McCool, D. M. Robinson, J. E. Sheats, G. C. Dismukes, *J. Am. Chem. Soc.* **2011**, *133*, 11446–11449.

[4] a) J. S. Kanady, R. Tran, J. A. Stull, L. Lu, T. A. Stich, M. W. Day, J. Yano, R. D. Britt, T. Agapie, *Chem. Sci.* **2013**, *4*, 3986–3996; b) A. Sartorel, M. Bonchio, S. Campagna, F. Scandola, *Chem. Soc. Rev.* **2013**, *42*, 2262–2280.

[5] a) A. Sartorel, M. Carraro, G. Scorrano, R. D. Zorzi, S. Geremia, N. D. McDaniel, S. Bernhard, M. Bonchio, *J. Am. Chem. Soc.* **2008**, *130*, 5006–5007; b) Y. V. Geletii, B. Botar, P. Kogerler, D. A. Hillesheim, D. G. Musaev, C. L. Hill, *Angew. Chem. Int. Ed.* **2008**, *47*, 3896–3899; *Angew. Chem.* **2008**, *120*, 3960–3963; c) Y. V. Geletii, Z. Huang, Y. Hou, D. G. Musaev, T. Lian, C. L. Hill, *J. Am. Chem. Soc.* **2009**, *131*, 7522–7523; d) Y. V. Geletii, C. Besson, Y. Hou, Q. Yin, D. G. Musaev, D. Quiñonero, R. Cao, K. I. Hardcastle, A. Proust, P. Kögerler, C. L. Hill, *J. Am. Chem. Soc.* **2009**, *131*, 17360–17370; e) A. Sartorel, P. Miró, E. Salvadori, S. Romain, M. Carraro, G. Scorrano, M. D. Valentin, A. Llobet, C. Bo, M. Bonchio, *J. Am. Chem. Soc.* **2009**, *131*, 16051–16053.

[6] R. Al-Oweini, A. Sartorel, B. S. Bassil, M. Natali, S. Berardi, F. Scandola, U. Kortz, M. Bonchio, *Angew. Chem. Int. Ed.* **2014**, *53*, 11182–11185; *Angew. Chem.* **2014**, *126*, 11364–11367.

[7] a) S. Berardi, G. La Ganga, M. Natali, I. Bazzan, F. Puntoriero, A. Sartorel, F. Scandola, S. Campagna, M. Bonchio, *J. Am. Chem. Soc.* **2012**, *134*, 11104–11107; b) F. Evangelisti, R. Guttinger, R. More, S. Luber, G. R. Patzke, *J. Am. Chem. Soc.* **2013**, *135*, 18734–18737; c) X. B. Han, Z. M. Zhang, T. Zhang, Y. G. Li, W. Lin, W. You, Z. M. Su, E. B. Wang, *J. Am. Chem. Soc.* **2014**, *136*, 5359–5366.

[8] X. B. Han, Y. G. Li, Z. M. Zhang, H. Q. Tan, Y. Lu, E. B. Wang, *J. Am. Chem. Soc.* **2015**, *137*, 5486–5493.

[9] A. M. Ullman, Y. Liu, M. Huynh, D. K. Bediako, H. Wang, B. L. Anderson, D. C. Powers, J. J. Breen, H. D. Abruna, D. G. Nocera, *J. Am. Chem. Soc.* **2014**, *136*, 17681–17688.

[10] a) N. Cox, D. A. Pantazis, F. Neese, W. Lubitz, *Acc. Chem. Res.* **2013**, *46*, 1588 – 1596; b) J. J. Stracke, R. G. Finke, *ACS Catal.* **2014**, *4*, 909 – 933.

[11] a) Q. Yin, J. M. Tan, C. Besson, Y. V. Geletii, D. G. Musaev, A. E. Kuznetsov, Z. Luo, K. I. Hardcastle, C. L. Hill, *Science* **2010**, *328*, 342 – 345; b) M. Murakami, D. Hong, T. Suenobu, S. Yamaguchi, T. Ogura, S. Fukuzumi, *J. Am. Chem. Soc.* **2011**, *133*, 11605 – 11613; c) Z. Huang, Z. Luo, Y. V. Geletii, J. W. Vickers, Q. Yin, D. Wu, Y. Hou, Y. Ding, J. Song, D. G. Musaev, C. L. Hill, T. Lian, *J. Am. Chem. Soc.* **2011**, *133*, 2068 – 2071; d) P.-E. Car, M. Guttentag, K. K. Baldridge, R. Alberto, G. R. Patzke, *Green Chem.* **2012**, *14*, 1680; e) S. Goberna-Ferrón, L. Vigara, J. Soriano-Lopez, J. R. Galan-Mascaros, *Inorg. Chem.* **2012**, *51*, 11707 – 11715; f) G. Zhu, E. N. Glass, C. Zhao, H. Lv, J. W. Vickers, Y. V. Geletii, D. G. Musaev, J. Song, C. L. Hill, *Dalton Trans.* **2012**, *41*, 13043 – 13049; g) S. Tanaka, M. Annaka, K. Sakai, *Chem. Commun.* **2012**, *48*, 1653 – 1655; h) F. Song, Y. Ding, B. Ma, C. Wang, Q. Wang, X. Du, S. Fu, J. Song, *Energy Environ. Sci.* **2013**, *6*, 1170; i) J. W. Vickers, H. Lv, J. M. Sumliner, G. Zhu, Z. Luo, D. G. Musaev, Y. V. Geletii, C. L. Hill, *J. Am. Chem. Soc.* **2013**, *135*, 14110 – 14118; j) M.-P. Santoni, G. La Ganga, V. Mollica Nardo, M. Natali, F. Puntoriero, F. Scandola, S. Campagna, *J. Am. Chem. Soc.* **2014**, *136*, 8189 – 8192; k) H. Lv, J. Song, Y. V. Geletii, J. W. Vickers, J. M. Sumliner, D. G. Musaev, P. Kogerler, P. F. Zhuk, J. Bacsa, G. Zhu, C. L. Hill, *J. Am. Chem. Soc.* **2014**, *136*, 9268 – 9271; l) R. Xiang, Y. Ding, J. Zhao, *Chem. Asian J.* **2014**, *9*, 3228 – 3237.

[12] L. Lisnard, P. Mialane, A. Dolbecq, J. Marrot, J. M. Clemente-Juan, E. Coronado, B. Keita, P. de Oliveira, L. Nadjo, F. Secheresse, *Chem. Eur. J.* **2007**, *13*, 3525 – 3536.

[13] Y. Umena, K. Kawakami, J. R. Shen, N. Kamiya, *Nature* **2011**, *473*, 55 – 60.

[14] M. Suga, F. Akita, K. Hirata, G. Ueno, H. Murakami, Y. Nakajima, T. Shimizu, K. Yamashita, M. Yamamoto, H. Ago, J. R. Shen, *Nature* **2015**, *517*, 99 – 103.

[15] T. Mathew, *J. Catal.* **2002**, *210*, 405 – 417.

[16] G. Zhu, Y. V. Geletii, P. Kogerler, H. Schilder, J. Song, S. Lense, C. Zhao, K. I. Hardcastle, D. G. Musaev, C. L. Hill, *Dalton Trans.* **2012**, *41*, 2084 – 2090.

[17] Y. Yamada, K. Yano, D. Hong, S. Fukuzumi, *Phys. Chem. Chem. Phys.* **2012**, *14*, 5753 – 5760.

[18] P. K. Ghosh, B. S. Brunschwig, M. Chou, C. Creutz, N. Sutin, *J. Am. Chem. Soc.* **1984**, *106*, 4772 – 4783.

[19] D. Hong, J. Jung, J. Park, Y. Yamada, T. Suenobu, Y.-M. Lee, W. Nam, S. Fukuzumi, *Energy Environ. Sci.* **2012**, *5*, 7606.

[20] A. C. Stewart, D. S. Bendall, *Biochem. J.* **1980**, *188*, 351 – 361.

Received: April 8, 2015
Revised: May 15, 2015
Published online on June 30, 2015